ORIGINAL

CrossMark

Experimental investigation on heat transfer characteristics of an oblique finned microchannel heat sink with different channel cross sections

R. Vinoth[1] · D. Senthil Kumar[2]

Abstract

The heat transfer and flow characteristics of oblique finned microchannel heat sink with a dimension of 48×80 mm^2 were investigated experimentally with different channel cross-sections. The three-channel cross sections were namely trapezoidal, square and semi-circle is analyzed by using Al_2O_3/water nanofluid with 0.25% volume fraction and water as a coolant. The experiments were performed with a constant mass flow rate of 0.1 LPM and varying heat flux ranging from 5.5 to 26.5 kW/m^2. The temperature and pressure drop across the inlet and outlet of the microchannel heat sink were measured to obtain heat and flow characteristics. The result shows that trapezoidal cross-section performs better and it provides 8.5 and 10.3% increased heat transfer rate than square and semi-circle cross sections respectively. Similarly, it gives 6.6 and 8.2% increase in friction factor than square and semi-circle respectively. Also, the case with trapezoidal cross-section creates lesser thermal resistance and slightly higher pumping power among the three sections.

Nomenclature

D	Diameter (m)
f	Friction Factor
h	Heat transfer coefficient(W/m^{2}K)
k	Thermal conductivity (W/mK)
L	Length(m)
m	Mass (kg)
Nu	Nusselt number
P	Pressure(Pa)
Q	Heat transfer(kJ)
q″	Channel heat flux (W/m^2)
R	Thermal resistance (K/W)
T	Temperature(K)
w_g	Uncertainty in the temperature gradient (°C/m)
W_{ti}	Uncertainty in temperature (°C)
y_i	Position of the ith thermocouple (m)
$\bar{y}$	Average thermocouple position in measuring segment (m)

Greek symbols

Δ	Difference
φ	Volume concentration of nanofluid
ρ	Density(kg/m^3)
Ω	Pumping power (W)

Subscripts

bf	Base fluid
nf	Nanofluid
in	Inlet
out	Outlet
p	Particle
h	Hydraulic
MCHS	Microchannel heat sink

✉ R. Vinoth
   rvinomech@gmail.com

1 Department of Mechanical Engineering, Adhiyamaan College of Engineering, Hosur, Tamil Nadu, India

2 Department of Mechanical Engineering, Sona College of Technology, Salem, Tamil Nadu, India

1 Introduction

In the last few decades, the integrated level of the electronic devices has been rapidly increasing, along with this, the weight of the component has been decreasing. It has led to higher heat flux produced by those parts due to less area of contact with atmospheric air. There has been also an increase in the failure rate of the element due to overheating.In order to reduce the failure rates; the effective and feasible method of thermal management is required immediately with less weight to maintain safe temperature limits of the components. These requirements led to the invention of the microchannel heat sink by varying heat flux. Microelectronic devices, which involve a variety of applications such as servers, PCs, laser diodes, and RF

devices, are continuously producing the heat flux density requirements from minimum to higher levels. It seemed to be an impossibly high limit of 200 W/cm^2 of heat dissipation in 1993 but now it appears to be a feasible target. The new challenge for this generation is in the range of heat flux between 600 and 1000 W/cm^2. Various heat sink configuration designs by many researchers have been discussed as follows.Jingru Zhang et al. [1] evaluated the flow and heat transfer in two different setups of the straight and U-shaped channel by using silicon as a substrate material. It was observed that the thermal resistance and pressure drop is higher in U-shaped microchannel than the straight channel, due to the mixing of flow.Wan et al. [2] presented the flow and heat transfer analysis along with a porous microchannel and concentrated on the Nusselt number and thermal resistance where the thermal resistance decreases with the increase in the heat flux that is being supplied. A Yan Fan et al. [3] studied a significant comparison of the oblique fin with the straight fin channels, and the study showed that the average Nusselt number increased by 75.1%. M. Naraki et al. [4] the studies about the overall heat transfer coefficient in microchannels with nanofluids. The results confirm that the heat transfer coefficient decreases with the increase in the inlet temperature. Mat Tokit et al. [5] investigates the optimized interrupted microchannel for the thermal performance. Interruptedmicrochannel heats sink (IMCHS) using nanofluids as working fluids are analyzed numerically to increase the heat transfer rate. The results were found to be 1.23 to 0.34% of penalty on the pressure drop in the IMCHS for Reynolds number ranging from 140 to 1034.Inan experimental aspect. Mohammad Kalteh et al. [6] studied that the nusselt number and nanofluid concentration are some of the important characteristics that influence the heat transfer. There is a significant value of 12.61% for the water and 7.42% in the 0.1% volume concentration alumina-water nanofluid for the deviation between experimental and numerical. Pawan K. Singh et al. [7] discussed the addition of the nanoparticles in the working fluid to increase the performance of the microchannel. There is only negligible fall in the pressure drop when compared with the percentage of increase in the heat transfer. H.A. Mohammed et al. [8] focused on the different nanofluid being used and compared with various other working fluids. The paper states clearly about the inlet cross-section with the trapezoidal being utilized in the experiment and Numerical analysis. Thermal resistance and pumping power are also influence the performance of microchannel [9–12]. GongnanXie et al. [9] discussed the unit thermal resistance and pumping power as essential characteristics. It was concluded that the counterflow experiences higher thermal resistance than the parallel flow and also the pumping power required for the counter flow is far greater than the parallel flow. According to Selvakumar et al. [10], the pumping power significantly

affects the flow characteristics of nanofluid in the microchannel. The pumping power of the nanofluid increases gradually with the increase in volume flow rate. There is an average rise of 15.11% of pumping power compared to DI water with that of 0.2% concentration nanofluid and concludes that this can be used for the further applications. Han-Chieh Chiu et al. [11] investigated the heat transfer performance, and the characteristics of the liquid cooling microchannel heat sink both experimentally and numerically. The effective thermal resistance was studied based on the porosity of the microchannel and was found that the porosity affects it about 50–75%. Tu-Chieh Hung et al. [12] carried out an experimental and numerical investigation of the different geometric configurations for the microchannel to select the better performing channel. The paper compared the thermal resistance with the pumping power to show the best-optimized microchannel that uses less power in both the cases. The thermal resistance seems to be decreased when the pumping power is increased, but the increase in it may cause disadvantage. Thus the optimized value of the pumping power and the thermal resistance was found to be 2 W with 0.06 K/W respectively. Vinoth et al. [13] discussed the heat and flow characteristics of three channel cross-sections.the water and Al_2O_3 nanofluids being used as-as coolant with 0.25% concentration. The oblique finned microchannel heat sink was tested by varying mass flux. The results showed that the trapezoidal cross-section gives better in heat transfer than square and semicircle cross-section due to which the nanoparticles added to the base fluid. Also, the trapezoidal attained highest friction factor due to rise in pressure drop. The investigation was carried out for the mass flow rate variation in the range of 0.1–0.5 lpm at constant heat flux. Certainly, the heat sink could not stay in constant heat load for a different application, it experiences the changes in heat flux. So, the varying of heat flux has been investigated in the present work to overcome the high heat dissipating problem. Predominantly, the microchannel heat sink plays a very significant role in dissipating the high heat flux. In a recent invention, up to 280 W of heat load has been removed at maximum temperature. Hence, proved that the present work has been done by varying the heat flux from 5.5–26.5 kW/m^2 to achieve a cooling effect for the reliability and improved lifetime of the electronic components.

Above literature review shows that there are several possible ways of changing channel cross section and coolant. In the present study, the heat and flow characteristics are being examined on the oblique finned Microchannel Heatsink (MCHS) with different channel cross section by flowing water and nanofluid. The study was preceded by both the nanofluid and water with all the three cross-sections. The study was carried out keeping constant mass flow rate and varying heat flux ranging from 5.5 kW/m^2, 10.5 kW/m^2, 15.6 kW/m^2,

20.88 kW/m^2 and 26.5 kW/m^2. Experiments were conducted for three cross sections of trapezoidal, square and semicircle and the results were compared.

2 Overall design

The schematic view of the oblique finned microchannel heat sink (MCHS) as shown in Fig. 1 with three channel cross sections namely semicircular cross-section, trapezoidal cross section, square cross section and overall view of oblique finned microchannel heat sink.

The oblique finned MCHS had an added advantage that where it has the oblique fins that improve the secondary flow. Thus there is more contact between the working fluid and the channel. The design also compact in size so that it can be accommodated everywhere. The different channel cross sections can also make an impact on the performance of the MCHS. The channel dimensions are 38.4cm^2, and the dimensions of microchannel heat sink with three cross sections are listed in Table 1.

3 Experimental study

3.1 Experimental setup

The schematic view of experimental flow loop is shown in Fig. 2. The hot fluid from the channel is passed on to the condenser (7) which cools the fluid for circulation. The fluid is stored in the reservoir (1) made up of stainless steel which can hold a capacity of 5–6 l. Filter made by Swagelok of 15 μm cross-section is mounted in mid-way between the reservoir and the pump. Gear pump (2) make by pedro Roquest capable up to 15 lpm. The gate valve (3) is located after the pump to regulate the flow. The flow meter (4) with the

Table 1 Geometric dimensions of microchannel with different channel cross-sections

Characteristic	Semicircular	Square	Trapezoidal
Channel, area (cm^2)	38.4	38.4	38.4
Main channel width, W_c(μm)	900	900	900
Fin width, W_w(μm)	900	900	900
Channel depth, H(μm)	900	900	900
Fin length, L (μm)	900	900	900
Fin pitch, P (μm)	800	800	800
Oblique angle, θ (deg)	26°	26 °	26 °

measurement range from 0.1 to 2 lpm make by sunshine model S-FM was utilized as the flow measuring device.

T-Type temperature sensor makes AMBETRONIC of range -20 °C to 200 °C is used to measure the temperature. The endpoint of the probe is placed in the channel and fluid to measure the temperature. It gives reading in a digital manner to the temperature data logger makes by AMBETRONICS model TC1600F of range -50 °C to 500 °C. The Datalogger (6) consists of eight channels with six probes are used. Pressure transducer made by SETRA model3100 ranges from 0 to 2 bars is used to measure inlet and outlet temperature and pressure of microchannel. The test section consists of oblique finned micro-channel made up of copper, and the channel section is covered by fiberglass. The test section consists of 7 temperature ports, each one at inlet and outlet and remaining 5 are utilized to determine the moderate temperatures. The pressure transducer is linked with a pressure data logger (6) make by AMBETRONICS model TC-800 ranging 0 to 5 bars which are used to visualize and record the pressure values. The heater is connected to an autotransformer in order keep the voltage constant which in turn provides the constant heat supply. The temperature and pressure sensor are connected to the computer via RS232 cable. The data logger continuously enables to take the temperature, and pressure readings and the

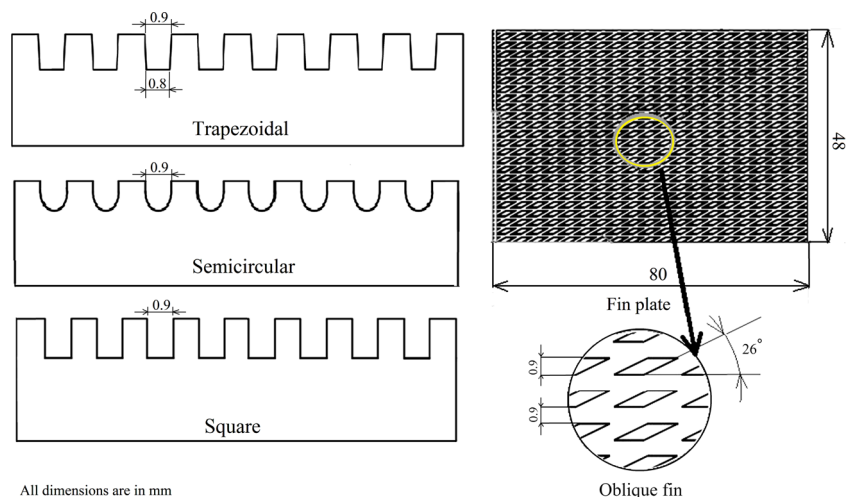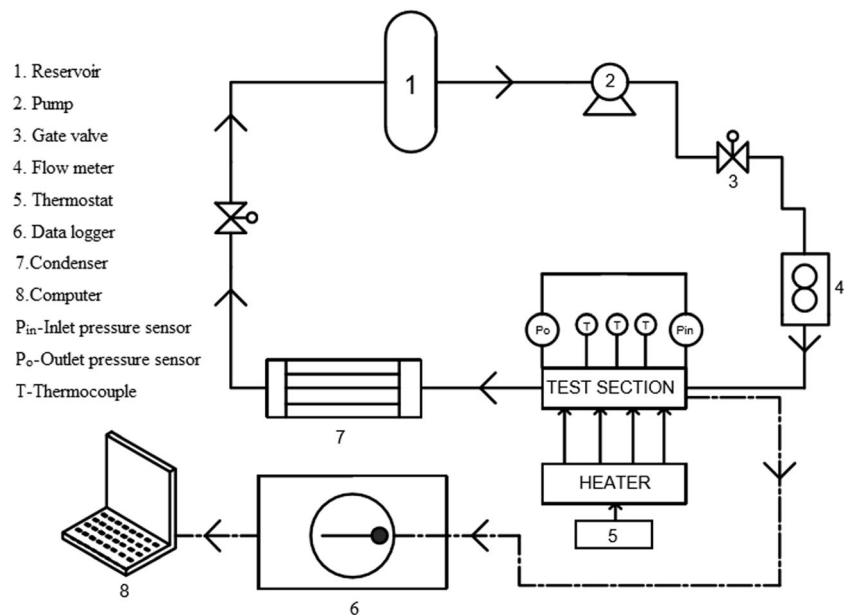**Fig. 1** Oblique finned microchannel heat sink with three channel cross sections

All dimensions are in mm

Fig. 2 Schematic flow loop for the experimental setup

1. Reservoir
2. Pump
3. Gate valve
4. Flow meter
5. Thermostat
6. Data logger
7. Condenser
8. Computer
P_{in}-Inlet pressure sensor
P_o-Outlet pressure sensor
T-Thermocouple

values are being plotted in a graph continuously. The pump runs with the help of 12 V battery to supply the water continuously, where the flow rate is controlled by using flow meter and needle valve.

3.2 Fabrication of test section setup

The test section consists of two parts namely base plate and the MCHS. The base plate was fabricated by CNC milling operation. The MCHS was first sized to the required thickness than the copper plate was sent to the EDM sparking and wire cutting for the production of the oblique fins. The rubber was used to insulate the base plate from the MCHS. The hose nipples of size 5 mm diameter were brazed with the microchannel base plate to connect the pipes to it. The holes of 4 mm diameter were drilled in the inlet, outlet and other random positions for fixing the temperature sensor probe. Then the glass was cut in the CNC machine for fixing it with

an interference fit on the top of the microchannel. Eventually, thermal adhesives were used to prevent leakage. Figure 3 shows the test section assembly of the oblique finned microchannel heat sink with the trapezoidal cross-section.

3.3 Nanofluid preparation

Nanofluid was prepared by mixing of calculated volume proportion of nanoparticles (Al_2O_3) in the base fluid of water. The volume proportion is taken as 0.25%. The nanoparticles and the water were mixed well with the help of the ultrasonic Johnson plastosonic. The mixture took 12 h to form a completely dispersed solution. The nanoparticles were at the average size of 45 nm. The nanofluid was found to be not sediment for 36 h, and therefore, no mixing is required further. Thus the nanofluid can be utilized in the experimental study.

Fig. 3 Test section assembly of the oblique finned microchannel heat sink

Fabricated fin plate
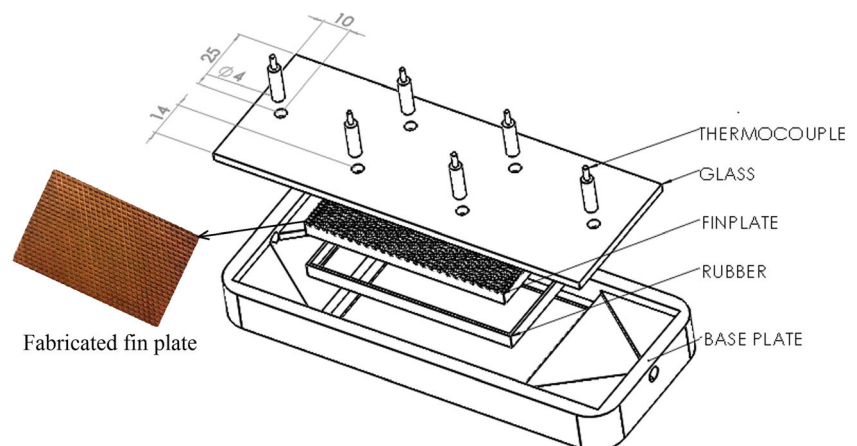
3.4 Thermophysical properties of nanofluid

The viscosity of the nanofluid plays a vital role in the pressure as well as the temperature values. Therefore to manipulate those values numerically, the viscosity is calculated via an empirical equation studied from the Pawan K. Singh et al. [7].

$$\mu_{nf} = \mu_{bf}(1 + 2.5\,\varphi)\left[1 + g\left(\frac{a}{d}\right)^{-2\varepsilon}\varphi^{2/3(\varepsilon+1)}\right] \quad (1)$$

Where $\varepsilon = -1/4$ and $g = 280$ taken arbitrarily for the alumina in water nanofluid.

Changwei Pang et al. [14] measured the thermal conductivity of nanofluids, base fluid valued are used to determine the nanofluid value. The thermal conductivity of nanofluids can be calculated by

$$knf = \frac{k_p + 2k_{bf} + 2(k_p - k_{bf})\varphi}{k_p + 2k_{bf} - (k_p - k_{bf})\varphi} \quad (2)$$

The heat capacity equation stated by the Tu-Chieh Hung et al. [15] was used to solve the governing equation; the equation is given below,

$$C\rho nf = \frac{(1-\varphi)(\rho C_p)_{bf} + \varphi(\rho C_p)_p}{\rho_{nf}} \quad (3)$$

The density of the nanofluid is estimated from the work of H.A. Mohammed et al. [8].

$$\rho_{nf} = (1-\varphi)\rho_{bf} + \varphi\rho_p \quad (4)$$

3.5 Experimental procedure

The heater requires 20–25 min to obtain the steady state with the help of the autotransformer by supplying power. Initially, the test section was checked for the leakage by flowing water as a coolant. The temperature sensor was ensured for correct working with the flow of water and nanofluid. The water flow rate was kept constant at 0.1 kg/min during start with the adjustment of the flow meter and the gate valve. The water removes a certain amount of heat from the channel for given period until steady state is obtained. The data loggers have used embedding with the computer for the continuous assessment. Thus the parameters like temperature and pressure are taken for determining the results. Then the autotransformer is adjusted from 5.5 kW/m², 10.5 kW/m², 15.66 kW/m², 20.8 kW/m² and 26.5 kW/m² and the readings are taken subsequently. The similar procedure is followed for other cross-sections also.

3.6 Uncertainty analysis

The uncertainty of the measurement of the channel dimension, pressure, and voltage can be taken as the least count of the corresponding measurement devices ±12 μm, ±0.1 Pa, and ± 0.1 V respectively. The uncertainties in temperature gradients (w_g) are calculated by the following equation given by Melanie Derby et al. [16].

$$w_g = \sqrt{w_n^2 + \left(\frac{q''D_-}{6k}\right)^2}\sqrt{\frac{1}{\sum_{i=1}^{N}(y_i - \bar{y})^2}} \quad (5)$$

The wall and fluid temperature uncertainties were determined to be ±0.03 °C. The uncertainties accompanying the heat transfer coefficient, and wall heat flux is assessed to be 2.2–4% and 1.8–3%, respectively. Also, the uncertainties reported on the pressure measurement found to be 3%. Steady-state prevails the maximum uncertainty of sensible heat gain by the fluid is 10% and the revealed maximum uncertainty of the heat transfer coefficient to be 18.5 W/m² K.

3.7 Experimental data post-processing

The heat transferred by the micro-channel can be calculated from inlet and outlet temperatures. The heat transfer equation is

$$Q = mc(T_{out} - T_{in}) \quad (6)$$

Here c is the specific heat capacity.

The average nusselt number is calculated using the following equation

$$Nu = \frac{h_{exp}D_h}{k} \quad (7)$$

The value of hydraulic diameter (D_h) for trapezoidal, square and semicircle is 0.9 mm.

Reynolds number, (Re)

$$Re = \frac{VD}{\mu} \quad (8)$$

The Reynolds number (Re) is 175 and the flow velocity, (V) is 0.15 m/s.

The pressure drop

$$\Delta p = p_{in} - p_{out} \quad (9)$$

The thermal resistance and pumping power was calculated using Minghou Liu et al. [17]

Thermal Resistance was calculated by,

$$R = \frac{T_s - \left(\dfrac{T_{in} + T_{out}}{2}\right)}{Q} \qquad (10)$$

Where T_s is surface temperature.

Pumping power was calculated by using the formula,

$$\Omega = \Delta p \, V \qquad (11)$$

Where, V is volumetric flow rate.

The friction factor was calculated from the work of Yan Fan et al. [3]

$$f = \frac{D_h}{L} \frac{\Delta p}{0.5 \rho u^2} \qquad (12)$$

4 Results and discussion

In this current work, three channel cross-sections of the microchannel heat sink were investigated experimentally by keeping constant mass flow rate and varying heat flux. The parameter such as heat transfer rate, Nusselt number, friction factor, thermal resistance and pumping power was evaluated to study the heat and flow characteristics of oblique finned microchannel heat sink.

4.1 Validation

Before the experimental study, it is necessary to validate experimental setup and procedure by comparing with the existing experimental work of C.J.Ho and Sehgal [18, 19]. Initial test runs were carried out in experimental microchannel set-up for the water with different mass flow rate. Figure 4 shows the variation of nusselt number with Reynolds number obtained from the present and previous experimental results. The Nusselt number is calculated by using the correlation and compared with Reynolds number. The deviation is within the acceptable limits. So the present experimental setup can be used for the further experiments.

4.2 The outlet temperature variation

The outlet temperature variation can be found out by varying heat flux for three cross sections flowing water and nanofluid. The obtained results are plotted against the heat flux for the different cross section with water and nanofluid in Fig. 5. From the graph, it is evident that the outlet temperature increases with the heat flux. The growth is observed because of the higher temperature difference between the surface temperature and the fluid temperature exists. It is also seen that the
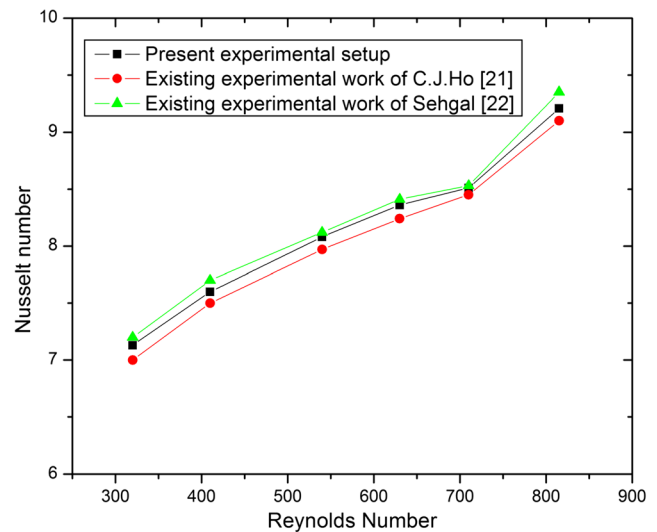

Fig. 4 Validation results for Nusselt number with Reynolds number

trapezoidal cross-section has higher outlet temperature compared to that of the other two cross-sections this is because of the higher contact area with the fluid.

4.3 Heat transfer coefficient characteristics

Heat transfer coefficient is one of the prominent characteristics while microchannel heat transfers study. The variations of heat transfer coefficient with respect to the heat flux have been predicted from Fig. 6. As a result, heat transfer coefficient increases with increase in heat flux. By comparing water and nanofluid, the nanofluid showed more significant effects with a trapezoidal cross-section. The result from the Fig. 6 clearly shows that the trapezoidal cross-section with water obtains higher than 5.87 and 13.10% of the square and the semicircle cross-sections respectively. Similarly, while flowing nanofluid, the trapezoidal channel achieves better results of
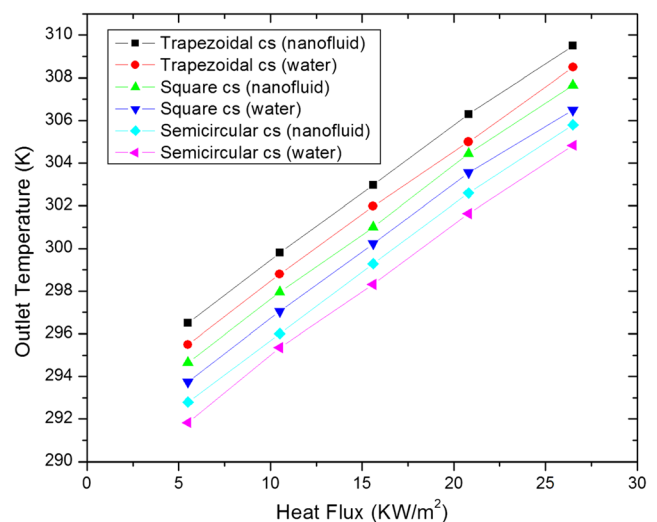

Fig. 5 Effect of heat flux on outlet temperature variation for different channel cross section and fluids
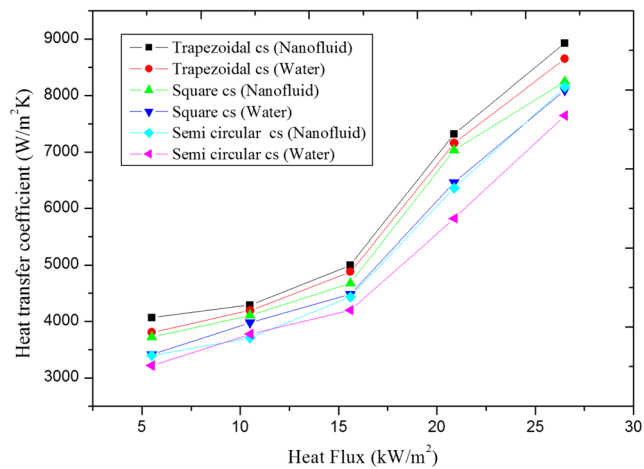
Fig. 6 Effect of heat flux on heat transfer coefficient variation for different channel cross section

13.42 and 14.29% than the square and the semicircle respectively. The heat transfer coefficient is also found to be higher for the nanofluid compared to that of the water. This is due to the higher thermal conductivity done by the solid nanoparticles. It can also be observed that the trapezoidal nanofluid exhibits better heat transfer coefficient compared to that of the other cross-sections. As trapezoidal cross section has larger wall area, effective entrance length and also influences more on the secondary flow.

4.4 Nusselt number characteristics

Variation of the Nusselt number is plotted against the heat flux in Fig. 7, and the Nusselt number increases since the convective heat transfer coefficient increases with the heat flux. In this, the trapezoidal cross-section has the higher Nusselt number than the other cross-sections. The trapezoidal attains 3D
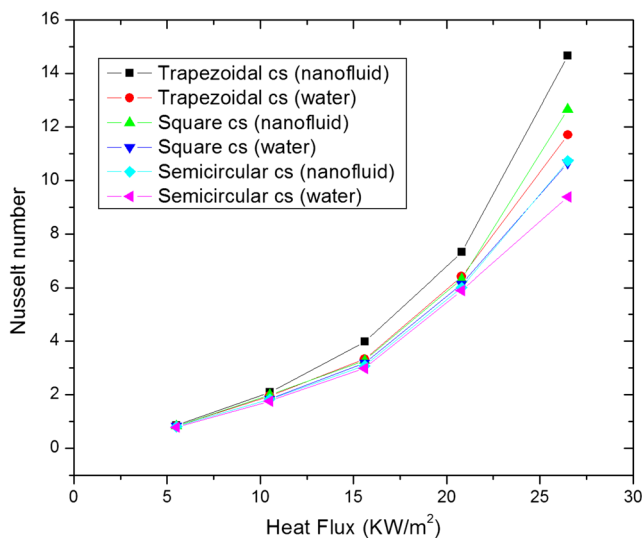
fluid mixing, that further enhances the rate of fluid flow. The Nusselt number also shows the similar effect as heat transfer rate and found to increase with the increase in the heat flux. The trapezoidal cross-section has the higher Nusselt number of 14.6 and 26.8% compared to the square and semicircle this is due to the higher secondary flow caused by its shape.

4.5 Thermal resistance characteristics

Thermal resistance versus the heat flux has been plotted in Fig. 8. The thermal resistance decreases with increases in heat flux, for all three cross-sections. But the thermal resistance of trapezoidal cross section is 3.2 and 4.5% which is lesser than the square and semi-circle respectively when water is the working fluid. It is revealed that if thermal resistance decreases the microchannel heat transfer rate will be enhanced. From the graph, it is evident that nanofluid creates less thermal resistance compared to that of the others. This is due to the higher thermal conductivity caused by the nanoparticles.

4.6 Effect of pumping power

Pumping power is one of the most undesirable characteristics of the microchannel heat sink. The increase in the performance of the microchannel is most often bought out by leaving behind the pumping power like improvement made by addition of nanoparticle. Fig. 9 shows the variation of pumping power with respect to mass flow rate. The pumping power of the semicircle cross-section is less compared to that trapezoidal and square. This is because fluid is sliding on the channel which decreases the pressure drop. The trapezoidal cross-section has slightly higher pumping power than the semicircle cross-section of 26.63%, and square cross-section has 23.60% by flowing water. Even though trapezoidal cross-
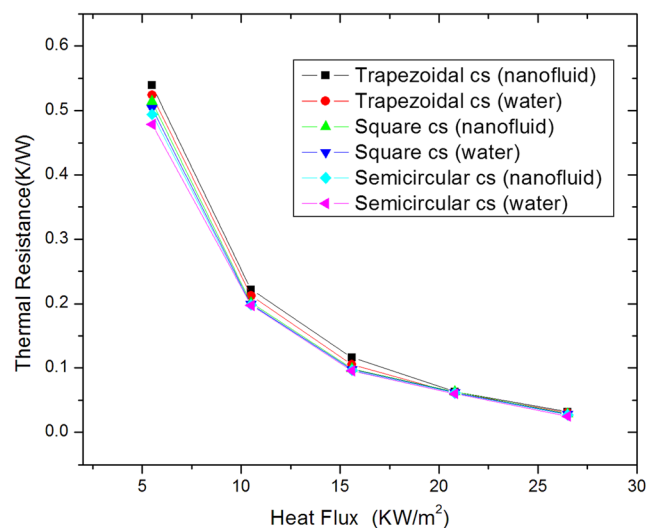

Fig. 7 Variation of heat transfer coefficient with heat flux for different channel cross section and fluids

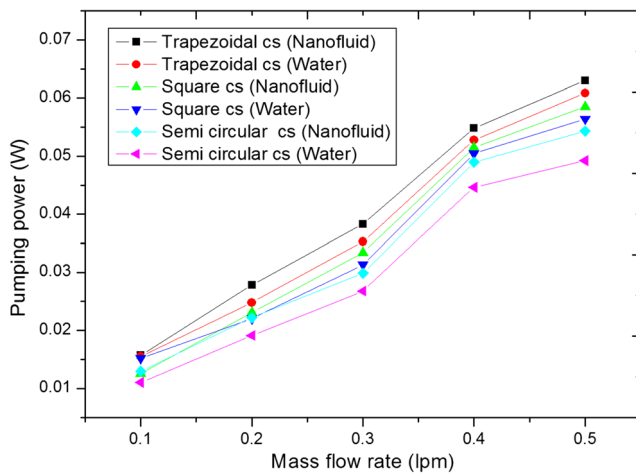Fig. 8 Thermal resistance versus heat flux for different channel cross section and fluids

Fig. 9 Effect of pumping power on mass flow rate for different channel cross section and fluids

sections require a little more pumping power than the other cross-section, it has good performance on heat transfer characteristics. From the Fig. 9, it is seen that semicircle has attained less pumping power due to fluid sliding over the surface, which decreases the pumping power of about 20.07% whereas, the trapezoidal and the square cross-section had only about 10.11 and 9.25%. The nanofluid requires higher pumping power than that water due to the high viscosity of nanofluid.

4.7 Friction factor characteristics

The friction factor is one of the primary flow characteristics studied in heat transfer study. It mainly depends on the secondary flow that occurs in the oblique finned microchannel heat sink. The Colburn factor is one of the most significant characteristics of microchannel heat sink. Figure 10 shows the variation of Colburn factor with friction factor. When the friction factor increases, the Colburn factor also decreases
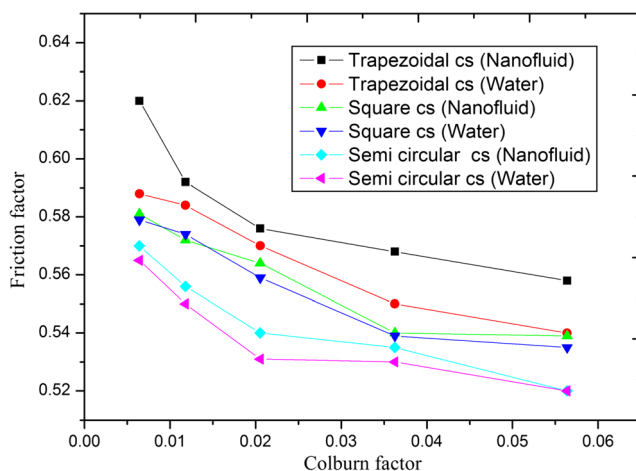

Fig. 10 The friction factor with Colburn factor for different channel cross section and fluids

simultaneously. The Colburn factor for the nanofluid is higher because of the particle present in the fluid. The Colburn factor for trapezoidal is still better for the case of water and nanofluid. The transitional flow regime was easily identified and differentiated from laminar and turbulent flow regime by plotting the local heat transfer coefficients in terms of a local Colburn factor. Hence the Colburn factor is the function of Reynolds number, Nusselt number, and Prandtl number. There is an increase of 1.65%, 1.72 and 1.77% between the three cross sections for flowing water and nanofluid. The Experimental friction factor for the trapezoidal cross-section is 6.6%, and 8.2% higher than the Square and semicircle respectively for water.

5 Conclusions

The experimental investigation has been carried out to study the effect of microchannel channel cross section using water and nanofluid by varying heat flux and keeping the Reynolds number as constant. Certainly, the heat sink could not stay in constant heat load from the application, it experiences the changes in heat flux. So, the varying of heat flux has been investigated in the present work to overcome the high heat dissipating problem. Based on the results the following conclusion has been summarized.

- The trapezoidal channel cross section shows the better heat and flow characteristics. It enhances heat transfer rate by 8.5 and 10.3% similarly friction factor by 6.6 and 8.2% higher than square and semi-circle respectively.
- The addition of nanoparticles to the base fluid, the heat transfer rate was found to be 4.6 and 8.6% higher than the square and semicircle.
- The thermal resistance decrease with increase in heat flux. Trapezoidal cross sections have a lesser thermal resistance of about 3.2 and 4.5% compared to the square and semi-circle cross-section.
- Trapezoidal cross section attains more pumping power than semicircle and square. However, it has better heat transfer characteristics.

References

1. Zhang J, Lin PT, Jaluria Y (2013) Design and optimization of multiple microchannel heat transfer systems. J Ther Sci Eng Appl 6:1–10
2. Wan ZM, Guo GQ, Su KL, Tu ZK, Liu W (2012) Experimental analysis of flow and heat transfer in a miniature porous heat sink for high heat flux application. Int J Heat Mass Transf 55:4437–4441

3. Fan Y, Lee PS, Jin L-W, BengWah C (2013) A simulation and experimental study of fluid flow and heat transfer on cylindrical oblique-finned heat sink. Int J Heat Mass Transf 61:62–72

4. Naraki M, Peyghambarzadeh SM, Hashemabadi SH, Vermahmoudi Y (2013) Parametric study of overall heat transfer coefficient of CuO/water nanofluids in a car radiator. Int J Therm Sci 66:82–90

5. Mat E, Tokit HAM, Yusoff MZ (2012) Thermal performance of optimized interrupted microchannel heat sink (IMCHS) using nanofluids. Int Commun Heat Mass Trans 39:1595–1604

6. Kalteh M, Abbassi A, Saffar-Avval M, Frijns A, Darhuber A, Harting J (2012) Experimental and numerical investigation of nanofluid forced convection inside a wide microchannel heat sink. Appl Therm Eng 36:260–268

7. Singh PK, Harikrishna PV, Sundararajan T, Das SK (2012) Experimental and numerical investigation into the hydrodynamics of nanofluids in microchannels. Exp Thermal Fluid Sci 42:174–186

8. Mohammed HA, Gunnasegaran P, Shuaib NH (2011) Influence of various base nanofluids and substrate materials on heat transfer in trapezoidal microchannel heat sinks. Int Commun Heat Mass Trans 38:194–201

9. Xie G, Liu Y, Sunden B, Zhang W (2013) Computational study and optimization of laminar heat transfer and pressure loss of double-layer microchannels for Chip liquid cooling. J Ther Sci Eng Appl 5(1):41–49

10. Selvakumar P, Suresh S (2012) Convective performance of CuO/water nanofluid in an electronic heat sink. Exp Thermal Fluid Sci 40:57–63

11. Chiu H-C, Jang J-H, Yeh H-W, Wu M-S (2011) The heat transfer characteristics of liquid cooling heatsink containing microchannels. Int J Heat Mass Transf 54:34–42

12. Hung T-C, Sheu T-S, Yan W-M (2012) Optimal thermal design of microchannel heat sinks with different geometric configurations. Int Commun Heat Mass Trans 39:1572–1577

13. Vinoth R, Senthil Kumar D (2017) Channel cross-section effect on heat transfer performance of oblique finned microchannel heat sink. Int Commun Heat Mass Trans 87:270–276

14. Pang C, Jung J-Y, Lee JW, Kang YT (2012) Thermal conductivity measurement of methanol-based nanofluids with Al_2O_3 and SiO_2 nanoparticles. Int J Heat Mass Transf 55:5597–5602

15. Hung T-C, Yan W-M, Wang X-D, Chang C-Y (2012) Heat transfer enhancement in microchannel heat sinks using nanofluids. Int J Heat Mass Transf 55:2559–2570

16. Derby M, Lee HJ, Peles Y, Jensen MK (2012) Condensation heat transfer in the square, triangular, and semi-circular mini-channels. Int J Heat Mass Transf 55:187–197

17. Liu M, Liu D, Xu S, Chen Y (2011) Experimental study on liquid flow and heat transfer in micro square pin fin heat sink. Int J Heat Mass Transf 54:5602–5611

18. Ho CJ, Wei LC, Li ZW (2010) An experimental investigation of the forced convective cooling performance of a microchannel heat sink with Al_2O_3/water nanofluid. Appl Therm Eng 30:96–103

19. Sehgal SS, Murugesan K, Mohapatra SK (2011) Experimental investigation of the effect of flow arrangements on the performance of a Micro-Channel heat sink. Exp Heat Transf 24:215–233